



# X-ray induced lock-in transition of cycloidal magnetic order in a multiferroic perovskite manganite

Y. Yamasaki,<sup>1,2</sup> H. Nakao,<sup>3</sup> Y. Murakami,<sup>3</sup> T. Nakajima,<sup>2</sup> A. Lafuente Sampietro,<sup>2,\*</sup> H. Ohsumi,<sup>4</sup> M. Takata,<sup>4</sup>  
T. Arima,<sup>2,5</sup> and Y. Tokura<sup>1,2</sup>

<sup>1</sup>*Department of Applied Physics and Quantum-Phase Electronics Center (QPEC), University of Tokyo, Tokyo 113-8656, Japan*

<sup>2</sup>*RIKEN Center for Emergent Matter Science (CEMS), Wako 351-0198, Japan*

<sup>3</sup>*Condensed Matter Research Center and Photon Factory, Institute of Materials Structure Science, High Energy Accelerator Research Organization, Tsukuba 305-0801, Japan*

<sup>4</sup>*RIKEN SPring-8 Center, Sayo, Hyogo 679-5148, Japan*

<sup>5</sup>*Department of Advanced Materials Science, University of Tokyo, Kashiwa 277-8561, Japan*

(Received 28 January 2015; revised manuscript received 3 March 2015; published 24 March 2015)

We report the x-ray photoexcitation effects on cycloidal magnetic order in a multiferroic perovskite-type manganite  $\text{Gd}_{0.5}\text{Tb}_{0.5}\text{MnO}_3$ . The material exhibits a competition between the  $P$  (electric polarization)|| $a$  ferroelectric state with the commensurate (C)  $ab$ -plane cycloidal and the  $P||c$  ferroelectric state with the incommensurate (IC)  $bc$ -plane cycloidal spin structure. The phase transition between these two phases can be induced by an application of a magnetic field. We found that the x-ray irradiation can induce the bidirectional and persistent phase transition between IC and C phases. The nonresonant x-ray magnetic diffraction revealed that both the initial and the x-ray induced phases have the  $bc$ -plane cycloidal magnetic structure, whereas the magnetic wave number varies between IC and C. The x-ray induced  $bc$ -plane cycloidal C phase is thus the hidden multiferroic phase in the  $\text{Gd}_{1-x}\text{Tb}_x\text{MnO}_3$  system, which does not show up with the application of any static field.

DOI: [10.1103/PhysRevB.91.100403](https://doi.org/10.1103/PhysRevB.91.100403)

PACS number(s): 75.85.+t, 61.05.cp

In recent years, there has been increasing interest in manipulations of magnetism without using a magnetic field aiming for the development of low-energy consumption spintronics. Along this line, there have been a number of studies in electric-field switching of magnetically ordered states in versatile magnetic systems, including diluted magnetic semiconductors and transition-metal oxides [1]. Among them, in multiferroics, i.e., materials with concurrent ferroelectric and magnetic orders, control of multiferroic domains is expected to be possible in terms of the application of an external field [2,3], such as magnetic control of ferroelectric polarization [4,5] and electric control of cycloidal spin helicity [6,7] and magnetization [8,9]. Furthermore, the attempts to control a multiferroic state by photoexcitation have recently been reported. One such experimental demonstration of photocontrol of multiferroic order is the laser-pulse (1.4 eV) induced switching from the paraelectric commensurate (C) spin collinear state to the ferroelectric incommensurate (IC) spin spiral in cupric oxide  $\text{CuO}$  [10]. It has been theoretically proposed that a short intense THz laser pulse could lead to a reorientation of cycloidal magnetic ordering via the excitation of electromagnons [11], which accompanies the rotation and reversal of the ferroelectric polarization. Related to this conjecture, the electromagnon activated by the THz electric field has been detected by the time-resolved resonant soft x-ray diffraction measurement in multiferroic  $\text{TbMnO}_3$  [12]. In this Rapid Communication, we study the effect of x-ray (high-energy photon) irradiation on the multiferroic phase transition.

Competing electronic orders near the phase boundary sometimes exhibit a significant response to external stimuli such as photoexcitation. Indeed, various photoinduced phase transitions have been discovered in transition-metal

oxides characterized by strongly correlated  $d$  electrons with spin, charge, and orbital degrees of freedom [13], such as  $\text{Pr}_{1-x}\text{Ca}_x\text{MnO}_3$  [14] and  $\text{V}_{1-x}\text{W}_x\text{O}_2$  [15]. In this Rapid Communication, we investigate x-ray irradiation effects on a multiferroic manganite  $\text{Gd}_{0.5}\text{Tb}_{0.5}\text{MnO}_3$ , which exhibits a keen competition between two ferroelectric states. In the perovskite manganite  $\text{RMnO}_3$  ( $R$  = rare earth) system, the spins on the Mn atoms take different ordering patterns depending on the temperature and magnitude of  $\text{GdFeO}_3$ -type lattice distortion [16]. One of the magnetically ordered phases of  $\text{TbMnO}_3$  shows a  $bc$ -plane cycloidal spin structure with an IC ordering wave vector  $(0\ q_m\ 1)$  with  $q_m \sim 0.27$  [4,6,17]. The  $bc$ -plane spin cycloid with propagation along the  $b$  axis generates ferroelectric polarization ( $P$ ) along the  $c$  axis ( $P||c$ ) that can be elucidated by the inverse Dzyaloshinskii-Moriya interaction (DMI) or spincurrent mechanism [18,19]. As the lattice distortion is varied by using solid solution  $\text{Gd}_{1-x}\text{Tb}_x\text{MnO}_3$  [20], the  $90^\circ$  reorientation of the cycloid from in the  $bc$  plane to in the  $ab$  plane occurs at around  $x = 0.4$  [see Figs. 1(a) and 1(b)]. The  $ab$ -cycloid spin structure, which has a C wave vector of  $q_m = 0.25$ , shows polarization along the  $a$  axis ( $P||a$ ) due to the IDM mechanism [21]. Here, we demonstrate the third hidden state ( $bc$ -plane cycloidal C order with  $P||c$ ) that can be generated by x-ray irradiation.

A single crystal of  $\text{Gd}_{0.5}\text{Tb}_{0.5}\text{MnO}_3$  was grown by a floating-zone technique. The synchrotron x-ray diffraction measurement for the superlattice structures, in which the photon energy was tuned to 12.0 keV, was performed at BL-3A in Photon Factory, KEK, Japan. The nonresonant x-ray magnetic diffraction, in which the photon energy was tuned to 12.6 keV, was studied at BL19LXU in SPring-8, Japan [22]. For these measurements, the crystal was cooled using a He-flow cryostat.

As shown in Fig. 1(c),  $\text{Gd}_{0.5}\text{Tb}_{0.5}\text{MnO}_3$  shows a ferroelectric phase transition at 24 K with electric polarization along the  $c$  axis ( $P||c$ ), whereas there is no ferroelectric

\*Present address: Univ. Grenoble Alpes, Grenoble, France and CNRS, Institut Néel, F-38042 Grenoble, France.

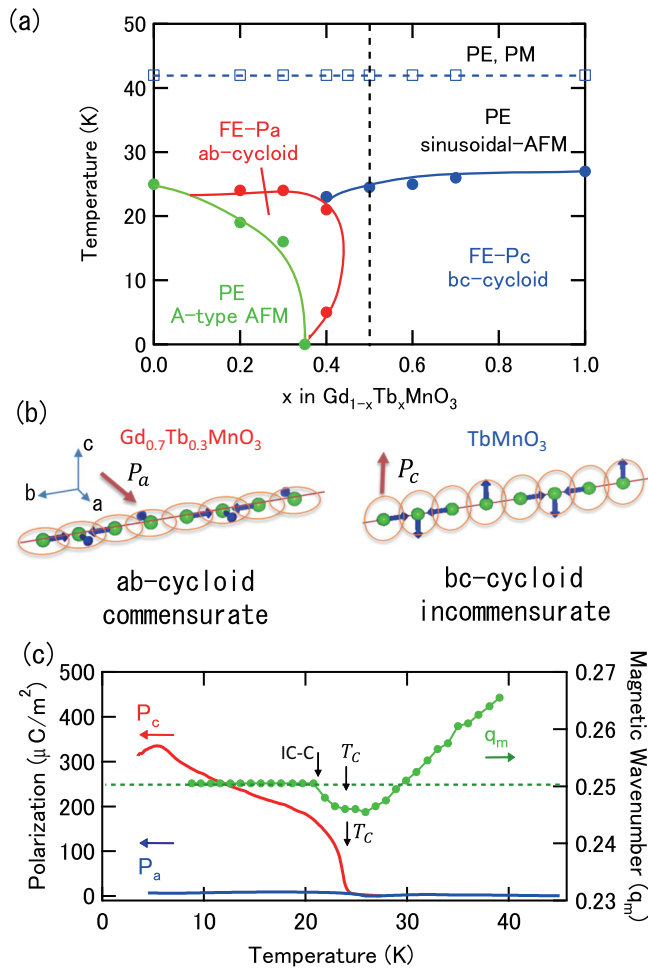


FIG. 1. (Color online) (a) Magnetic and ferroelectric phase diagram of  $Gd_{1-x}Tb_xMnO_3$  in the  $x$ - $T$  plane. Here, the abbreviations respectively represent paraelectric (PE), paramagnetic (PM), ferroelectric (FE), and antiferromagnetic (AFM) phases. (b) Magnetic structures of Mn spins in the  $ab$ -plane cycloidal commensurate phase of  $Gd_{0.7}Tb_{0.3}MnO_3$  (left) and in the  $bc$ -plane cycloidal incommensurate phase of  $TbMnO_3$  (right). (c) Temperature dependence of ferroelectric polarizations along the  $a$  axis ( $P_a$ ) and the  $c$  axis ( $P_c$ ) measured without x-ray irradiation, and the magnetic wave number  $q_m$  measured with x-ray irradiation.

polarization component along the  $a$  axis ( $P||a$ ) down to the lowest temperature [20]. Figure 1(c) also shows the temperature dependence of the magnetic wave number  $q_m$  obtained by the superlattice peak position of  $(0\ 4 - q_l\ 1)$  reflection [23]. The temperature-scan measurement was done after the prolonged-time ( $> 10$  min) x-ray irradiation at 8 K. As the temperature decreases, the compound shows an IC wave number  $q_m = 0.247$  below the critical temperature of the  $P||c$  ferroelectric phase, and then undergoes an IC-C transition from  $q_m = 0.247$  to  $q_m = 0.25$  at around 20 K. However, upon the IC-C transition, which was detected by the synchrotron x-ray measurement, there is no discerned anomaly in the ferroelectric polarization, measured without x-ray irradiation. This puzzling observation led us to speculate that the observed IC-C transition may occur only with the assist of the x-ray irradiation.

To make the effect of x-ray irradiation clear, we have examined the x-ray irradiation time dependence of the superlattice diffraction intensity at the commensurate  $(0\ 3.5\ 1)$  and the incommensurate  $(0\ 3.507\ 0)$  reflections. In this experiment, the x-ray irradiation was turned off during temperature variation until the start of measurements. In exposing the sample to x rays at 10 K, the diffraction intensity of the C phase increases, whereas that of the IC phase conversely decreases. This behavior indicates that the majority of the domains are initially in the IC phase and that the prolonged x-ray irradiation ( $> 10$  min) can wholly change the magnetic order from the IC to the C state. In contrast, when the magnetic ordering is fully converted to the C states by x-ray excitation at 10 K and then the temperature is elevated without x-ray irradiation up to 23 K, the x-ray induced phase transition is observed in the counter direction, i.e., from the C to the IC states. In these experimental procedures, we have confirmed that the superlattice reflection intensity remains constant while x-ray irradiation is off, indicating that the temporal variation of the diffraction intensity originates from x-ray irradiation and not from the thermal relaxation. Measurements of the x-ray induced phase transition with varying incident x-ray photon flux revealed that the volume fraction of the x-ray induced phase can be scaled with the total dose of irradiating x-ray photons, being irrespective of the x-ray photon flux. Based on these results, we can estimate from the initial slope of the intensity in Fig. 2 that a few hundreds of Mn sites can be converted per one x-ray photon. Consequently,  $Gd_{0.5}Tb_{0.5}MnO_3$  exhibits the persistent and bidirectional x-ray induced phase transition between the C and the IC phases, whose direction is switched with varying temperature.

Figures 3(a) and 3(b) show the temperature dependence of the x-ray induced phase transition in the cooling and warming

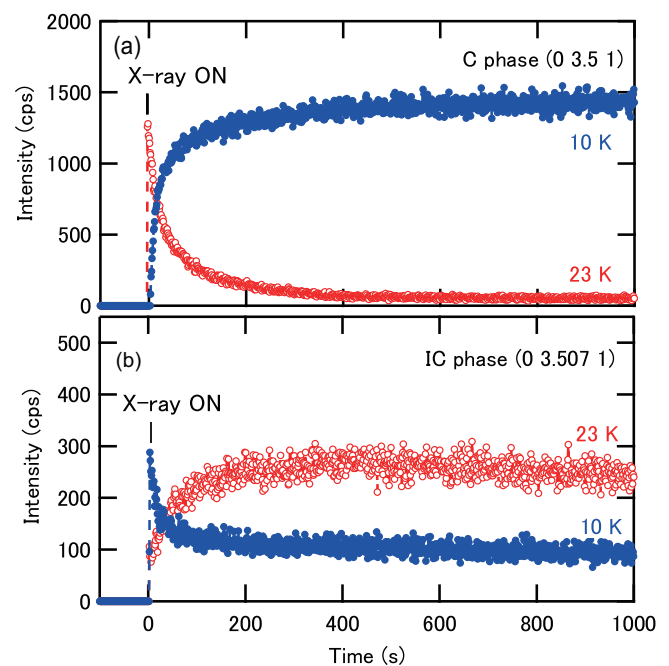


FIG. 2. (Color online) X-ray irradiation time dependence of superlattice diffraction intensities for (a) the C  $(0\ 3.5\ 1)$  reflections and for (b) the IC  $(0\ 3.507\ 1)$  reflections.

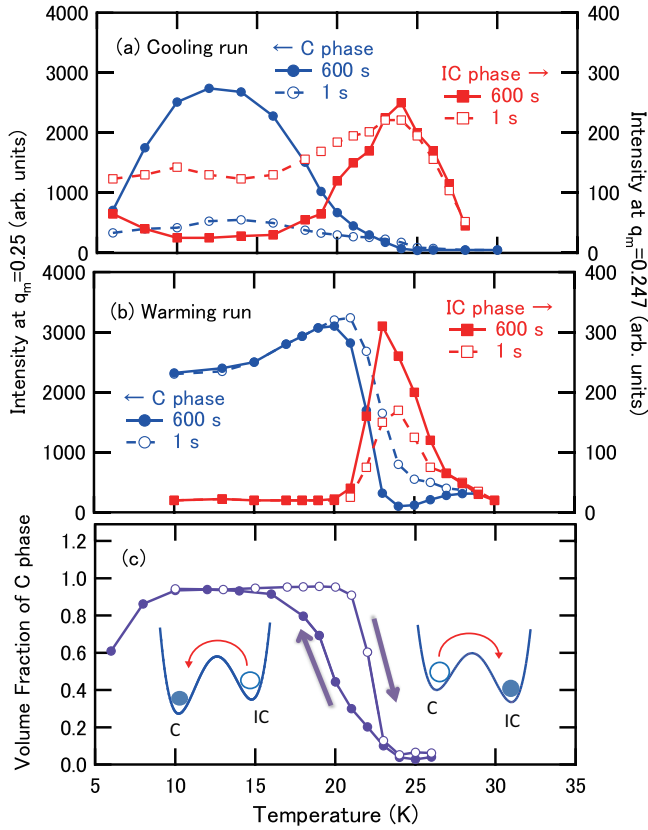


FIG. 3. (Color online) Temperature dependence of the superlattice reflection intensity of the C (0 3.5 1) and IC (0 3.507 1) phases taken with the acquisition times of 1 and 600 s in (a) a cooling run and (b) a warming run. (c) Temperature dependence of the volume fraction of the x-ray induced C phase. Arrows in (c) indicate the temperature scan direction. Insets in (c) represent schematic free energy diagrams and the x-ray induced phase transition below 23 K in the cooling run (left) and above 21 K in the warming run (right).

runs, respectively. In these figures, we plot the diffraction intensities observed with the acquisition time periods of 1 and 600 s at respective temperatures. The volume fraction of the x-ray induced C phase, as estimated from the 600 s data set of the C and IC reflections, is also depicted in Fig. 3(c). The x-ray induced phase transition from the IC to the C phase occurs below 24 K in the cooling process, and that from the C to the IC phase occurs between 20 and 27 K in the warming process. The observed temperature dependence evokes the presence of the double-well potential [24,25]; the phase transition occurs from the metastable state to the most stable state with the assist of x-ray irradiation, while without x ray the low-temperature IC-to-C transition appears to be largely suppressed by a high potential barrier. The initial state could be a metastable state as determined by the experimental process, and the final state produced by x-ray irradiation may be a thermodynamic equilibrium state as determined by the energy level between the IC phase and the C phase. The observed switching of the direction of x-ray phase transition between the IC and the C states can be elucidated by postulating an alternation of the most stable state with varying temperature.

We have measured nonresonant x-ray magnetic scattering to determine the magnetic ordering structure in the x-ray

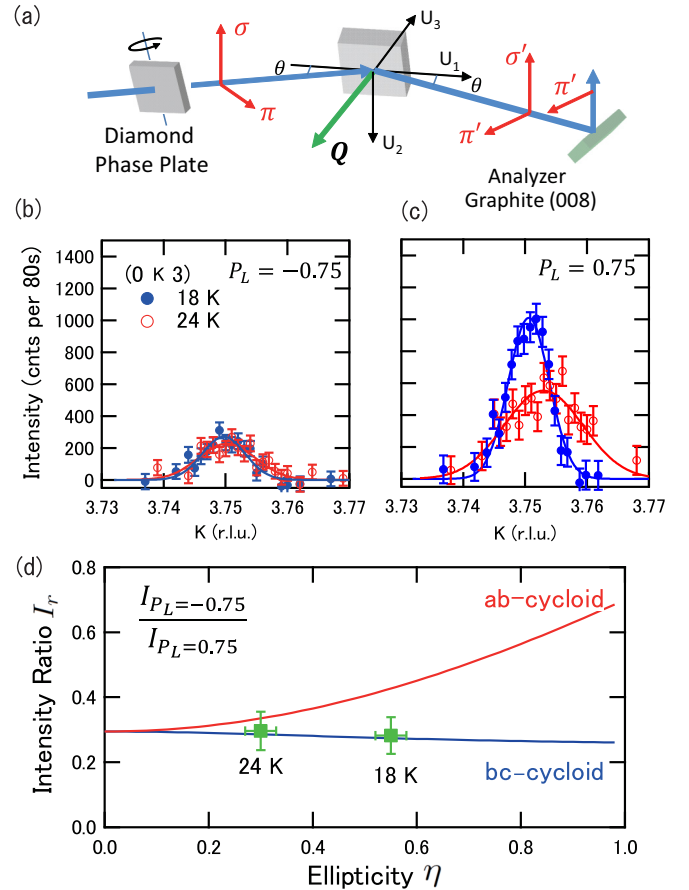


FIG. 4. (Color online) (a) Schematic figure of the experimental setup for the nonresonant x-ray diffraction with tuning the incident x-ray polarization by a phase plate and analyzing the diffracted x-ray polarization by a graphite single crystal. Nonresonant x-ray magnetic diffraction measured at 18 and 24 K for (b)  $P_L = -0.75$  and for (c)  $P_L = 0.75$ . Here,  $P_L$  stands for the presentation of incident x-ray polarization, for which definition see the text. (d) The simulated results for the *ab*-plane and *bc*-plane cycloidal magnetic ordering in comparison with the ratio of the measured intensity  $I_{P_L=-0.75}/I_{P_L=0.75}$  with the change of the parameter of the spin cycloid ellipticity.

induced phases. X rays can respond not only to charge but also to magnetic moment in condensed matter [26–28]. Since the x-ray susceptibility of magnetic moment has to be treated as a tensor, the direction of magnetic moment can be estimated by the polarization analysis of the scattering process. In the present experiment, as shown in the experimental setup of Fig. 4(a), the polarization of scattered x rays from the sample was analyzed by a pyrographite crystal using (008) reflection. The analyzer crystal was set to measure the  $\pi'$ -polarized scattered x rays selectively. In addition, the polarization of incident x rays was tuned with a diamond phase plate between  $\pi$  and  $\sigma$  polarization. The polarization of incident x rays is parametrized as  $P_L = \cos \delta$ , where  $\delta$  is the phase of the light wave and appears in the Jones vector of x ray as  $(E_\sigma, E_\pi) = \frac{1}{2}(1 + e^{i\delta}, 1 - e^{i\delta})$ . Figures 4(b) and 4(c) show the nonresonant x-ray magnetic diffraction profiles for (0 4 -  $q_m$  3) reflection with the scattering plane aligned along the [100] direction, measured at 18 and 23 K, where the fully x-ray induced phase is the C phase and the IC phase, respectively. The

magnetic diffraction measured with the polarization parameter being  $P_L = \pm 0.75$ , which is the maximum tunable value of  $|P_L|$  in the present experimental setting. To determine the spin cycloidal plane the diffraction intensity ratio  $I_r = I_{P_L=-0.75}/I_{P_L=0.75}$  was analyzed as a function of spin ellipticity  $\eta$ , which is defined as  $\eta = m_a/m_b$  ( $m_c/m_b$ ) in the  $ab$ - ( $bc$ -) cycloid magnetic structure [29]. As shown in Fig. 4(d), the intensity ratio increases (decreases) with increasing  $\eta$  for the  $ab$ - ( $bc$ -) cycloid phase. The experimental results measured at the IC (23 K) and C (18 K) phases are also plotted in Fig. 4(d), which show good agreement with the calculated value for the  $bc$ -cycloid magnetic structure. Here, the ellipticity values are estimated from the results of polarized neutron scattering [21]. It indicates that the x-ray induced IC-C phase transition is not accompanied by the flop of the cycloid plane.

In all, three multiferroic phases—the  $bc$ -plane cycloid C, the  $ab$ -plane cycloid C, and the  $bc$ -plane cycloid IC phases—are revealed to show up in  $\text{Gd}_{0.5}\text{Tb}_{0.5}\text{MnO}_3$ . The irradiation of x ray triggers the phase transition between the  $bc$ -plane cycloid C and the  $bc$ -plane cycloid IC phase, while the application of a static magnetic field does between the  $ab$ -plane cycloid C and the  $bc$ -plane cycloid IC phase. The difference in phase transition behaviors between the x-ray irradiation and the application of a static magnetic field can be elucidated as follows. In perovskite-type  $\text{RMnO}_3$ , the magnetic-field induced reorientation of the cycloidal plane is theoretically reproduced by considering the energetical competition between the DMI, single-ion anisotropy and the effective field from the rare-earth  $f$  moment, which acts on the Mn spins via the  $f$ - $d$  coupling [30]. The applied magnetic field reduces the DMI energy and influences the  $f$ - $d$  interaction, and thereby controls the energetical competition; this may result in the concurrent conversion of the cycloidal plane and the magnetic wave number, as observed in the magnetic-field switching between the  $ab$ -plane cycloid C and the  $bc$ -plane cycloid IC in  $\text{Gd}_{0.5}\text{Tb}_{0.5}\text{MnO}_3$ . By contrast, the x-ray irradiation may not directly influence either the DMI or the  $f$ - $d$  interaction, and thus not change the free energy difference between the  $ab$ -plane cycloid C and  $bc$ -plane cycloid IC phases, but promote the phase transition from the

metastable state to the most stable state which would otherwise be suppressed by the presence of a potential barrier in changing temperature.

X-ray induced phenomena have been observed in some manganites, i.e., the x-ray induced persistent phase transition in charge-ordered manganites [31] and the x-ray induced ferroelectric domain manipulation in a multiferroic manganite [32]. It was argued that the x-ray irradiations may induce charge defects in the sample, which create a metastable state and/or an effective electric field. In the present case, such defects may also induce nonthermal spin disorder, resulting in a broad spectrum of magnetic excitation, which should include a phason mode of cycloid spin, and thus will drive the phase transition from the metastable spin-ordered state to the stable one.

In summary, we demonstrate the persistent and reversible phase transitions between the IC and C cycloidal magnetic state by x-ray irradiation in the multiferroic manganite  $\text{Gd}_{0.5}\text{Tb}_{0.5}\text{MnO}_3$ . The observed phase transition can be elucidated by postulating the two (meta-)stable magnetic structures separated by a potential barrier and the alternation of the most stable state with varying temperature. The nonresonant x-ray magnetic scattering measurement revealed that the irradiation induces the phase transition between the  $bc$ -plane cycloid C and the  $bc$ -plane cycloid IC phase. The photoinduced effect as observed in this study will provide a path for photocontrol of multiferroics.

The authors are grateful to D. Okuyama, Y. Yamaki, J. Yamaura, and R. Kumai for their enlightening discussions. This work was supported by Grants-in-Aid for Scientific Research from the Japan Society for the Promotion of Science (Grant No. 22740243). The Funding Program for World Leading Innovative R&D on Science and Technology (FIRST Program). The synchrotron radiation experiments were performed at BL-3A/4C in Photon Factory with the approval of the Photon Factory Program Advisory Committee (Proposals No. 2009S2-008, No. 2012S2-005, No. 2010G086, No. 2011G597, and No. 2013G733) and at BL19LXU in SPring-8 with the approval of RIKEN (Proposal No. 20140085).

- 
- [1] F. Matsukura, Y. Tokura, and H. Ohno, *Nature Nanotechnol.* (to be published).
- [2] S.-W. Cheong and M. Mostovoy, *Nat. Mater.* **6**, 13 (2007).
- [3] Y. Tokura, S. Seki, and N. Nagaosa, *Rep. Prog. Phys.* **77**, 076501 (2014).
- [4] T. Kimura, T. Goto, H. Shintani, K. Ishizaka, T. Arima, and Y. Tokura, *Nature (London)* **426**, 55 (2003).
- [5] Y. Yamasaki, S. Miyasaka, Y. Kaneko, J.-P. He, T. Arima, and Y. Tokura, *Phys. Rev. Lett.* **96**, 207204 (2006).
- [6] Y. Yamasaki, H. Sagayama, T. Goto, M. Matsuura, K. Hirota, T. Arima, and Y. Tokura, *Phys. Rev. Lett.* **98**, 147204 (2007).
- [7] H. Jang, J.-S. Lee, K.-T. Ko, W.-S. Noh, T. Y. Koo, J.-Y. Kim, K.-B. Lee, J.-H. Park, C. L. Zhang, S. B. Kim *et al.*, *Phys. Rev. Lett.* **106**, 047203 (2011).
- [8] Y. Tokunaga, Y. Taguchi, T.-h. Arima, and Y. Tokura, *Nat. Phys.* **8**, 838 (2012).
- [9] Y. S. Chai, S. Kwon, S. H. Chun, I. Kim, B.-G. Jeon, K. H. Kim, and S. Lee, *Nat. Commun.* **5**, 4208 (2014).
- [10] S. L. Johnson, R. A. de Souza, U. Staub, P. Beaud, E. Möhr-Vorobeva, G. Ingold, A. Caviezel, V. Scagnoli, W. F. Schlotter, J. J. Turner *et al.*, *Phys. Rev. Lett.* **108**, 037203 (2012).
- [11] M. Mochizuki and N. Nagaosa, *Phys. Rev. Lett.* **105**, 147202 (2010).
- [12] T. Kubacka, J. Johnson, M. Hoffmann, C. Vicario, S. De Jong, P. Beaud, S. Grübel, S.-W. Huang, L. Huber, L. Patthey *et al.*, *Science* **343**, 1333 (2014).
- [13] Y. Tokura, *J. Phys. Soc. Jpn.* **75**, 011001 (2006).
- [14] K. Miyano, T. Tanaka, Y. Tomioka, and Y. Tokura, *Phys. Rev. Lett.* **78**, 4257 (1997).
- [15] K. Shibuya, D. Okuyama, R. Kumai, Y. Yamasaki, H. Nakao, Y. Murakami, Y. Taguchi, T. Arima, M. Kawasaki, and Y. Tokura, *Phys. Rev. B* **84**, 165108 (2011).

- [16] T. Kimura, S. Ishihara, H. Shintani, T. Arima, K. T. Takahashi, K. Ishizaka, and Y. Tokura, *Phys. Rev. B* **68**, 060403 (2003).
- [17] M. Kenzelmann, A. B. Harris, S. Jonas, C. Broholm, J. Schefer, S. B. Kim, C. L. Zhang, S.-W. Cheong, O. P. Vajk, and J. W. Lynn, *Phys. Rev. Lett.* **95**, 087206 (2005).
- [18] H. Katsura, N. Nagaosa, and A. V. Balatsky, *Phys. Rev. Lett.* **95**, 057205 (2005).
- [19] M. Mostovoy, *Phys. Rev. Lett.* **96**, 067601 (2006).
- [20] T. Goto, Y. Yamasaki, H. Watanabe, T. Kimura, and Y. Tokura, *Phys. Rev. B* **72**, 220403 (2005).
- [21] Y. Yamasaki, H. Sagayama, N. Abe, T. Arima, K. Sasai, M. Matsuura, K. Hirota, D. Okuyama, Y. Noda, and Y. Tokura, *Phys. Rev. Lett.* **101**, 097204 (2008).
- [22] M. Yabashi, T. Mochizuki, H. Yamazaki, S. Goto, H. Ohashi, K. Takeshita, T. Ohata, T. Matsushita, K. Tamasaku, Y. Tanaka *et al.*, *Nucl. Instrum. Methods Phys. Res., Sect. A* **467-468**, 678 (2001).
- [23] The lattice modulation is derived from the spatial modulation of magnetic moment through the exchange striction and obeys a relation  $q_l = 2q_m$  in the lattice modulation vector  $(0\ q_l\ 0)$ .
- [24] N. Takubo, I. Onishi, K. Takubo, T. Mizokawa, and K. Miyano, *Phys. Rev. Lett.* **101**, 177403 (2008).
- [25] Y. Yamaki, Y. Yamasaki, H. Nakao, Y. Murakami, Y. Kaneko, and Y. Tokura, *Phys. Rev. B* **87**, 081107 (2013).
- [26] M. Blume and D. Gibbs, *Phys. Rev. B* **37**, 1779 (1988).
- [27] D. Mannix, D. F. McMorrow, R. A. Ewings, A. T. Boothroyd, D. Prabhakaran, Y. Joly, B. Janousova, C. Mazzoli, L. Paolasini, and S. B. Wilkins, *Phys. Rev. B* **76**, 184420 (2007).
- [28] H. Sagayama, N. Abe, K. Taniguchi, T.-h. Arima, Y. Yamasaki, D. Okuyama, Y. Tokura, S. Sakai, T. Morita, T. Komesu *et al.*, *J. Phys. Soc. Jpn.* **79**, 043711 (2010).
- [29] See Supplemental Material at <http://link.aps.org/supplemental/10.1103/PhysRevB.91.100403> for details of the calculation in the nonresonant x-ray diffraction.
- [30] M. Mochizuki and N. Furukawa, *Phys. Rev. Lett.* **105**, 187601 (2010).
- [31] M. Garganourakis, V. Scagnoli, S. W. Huang, U. Staub, H. Wadati, M. Nakamura, V. A. Guzenko, M. Kawasaki, and Y. Tokura, *Phys. Rev. Lett.* **109**, 157203 (2012).
- [32] E. Schierle, V. Soltwisch, D. Schmitz, R. Feyerherm, A. Maljuk, F. Yokaichiya, D. N. Argyriou, and E. Weschke, *Phys. Rev. Lett.* **105**, 167207 (2010).